Equation of state at finite baryon density based on lattice QCD

Pasi Huovinen[1] **and Péter Petreczky**[2]

[1] Institut für Theoretische Physik, Johann Wolfgang Goethe-Universität, 60438 Frankfurt am Main, Germany

[2]Physics Department, Brookhaven National Laboratory, Upton, NY 11973, USA

E-mail: huovinen@th.physik.uni-frankfurt.de

Abstract. We employ the lattice QCD data on Taylor expansion coefficients to extend our previous parametrization of the equation of state to finite baryon density. When we take into account lattice spacing and quark mass dependence of the hadron masses, the Taylor coefficients at low temperature are equal to those of hadron resonance gas. Thus the equation of state is smoothly connected to the hadron resonance gas equation of state at low temperatures. We also show how the elliptic flow is affected by this equation of state at the maximum SPS energy.‡

One of the methods to extend the lattice QCD calculations to non-zero chemical potential is Taylor expansion. In that approach pressure is Taylor expanded in chemical potentials, and the Taylor coefficients are calculated on the lattice at zero chemical potential. In this contribution we use the results of the most comprehensive lattice QCD analysis of the Taylor coefficients to date [1, 2] to construct a parametrization of an equation of state (EoS) for finite baryon density. As in our earlier parametrization of the EoS at zero chemical potential [3], we require that our parametrization matches smoothly to the hadron resonance gas (HRG) at low temperatures.

Taylor coefficients are simply derivatives of pressure with respect to baryon and strangeness chemical potential:

$$c_{ij}(T) = \frac{1}{i!j!}\frac{T^{i+j}}{T^4}\frac{\partial^i}{\partial\mu_B^i}\frac{\partial^j}{\partial\mu_S^j}P(T,\mu_B=0,\mu_S=0). \qquad (1)$$

Purely baryonic and strange coefficients are related to quadratic and higher order fluctuations of conserved charges, whereas mixed derivatives of pressure give correlations of these charges. The second order baryonic coefficient c_{20} is shown in the left panel of Fig. 1. The lattice result for c_{20}, as well as for all the other coefficients, is well below the HRG result obtained with physical masses (solid line). This discrepancy can largely be explained by the lattice discretization effects on hadron masses: When the hadron mass spectrum is modified accordingly (for details see [4]), the HRG model reproduces the lattice data. The dashed and dotted curves in Fig. 1 refer to different treatment of

‡ Talk given at Quark Matter 2011, 22-28 May 2011, Annecy, France

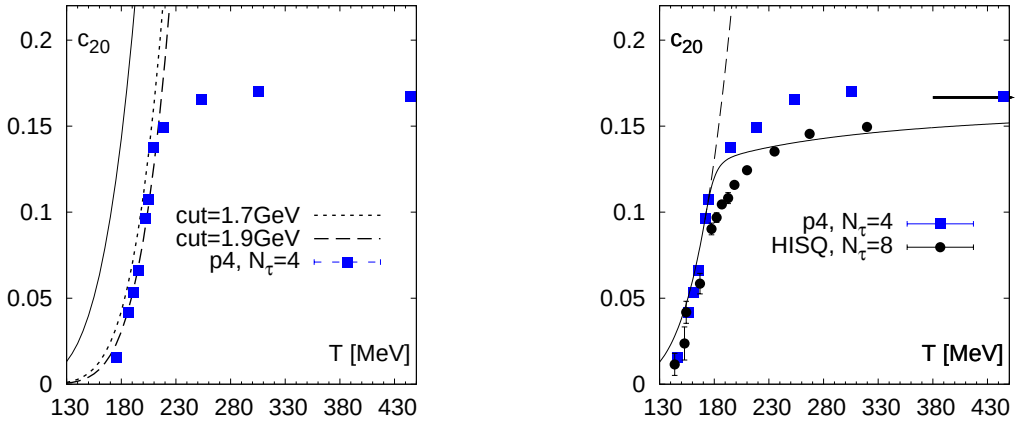

Figure 1. (Left) The second order baryonic Taylor coefficient c_{20} calculated on the lattice with p4 action [2] and compared with the HRG values with free particle (solid line) and lattice masses (dashed and dotted lines).
(Right) The parametrization (solid line) and HRG value (dashed) of the c_{20} coefficient compared with the shifted p4 data (see the text). The more recent lattice result with the HISQ action [5] is also shown. The arrow depicts the Stefan-Boltzmann value of c_{20}.

baryonic resonances. We modify their masses in the same way than ground state baryons up to a threshold m_{cut} but keep the masses of heavier resonances in their physical values. As seen, the exact value of this threshold has only a small effect on c_{20}.

Closer look at the HRG curves in Fig. 1 (left) reveals that the incorporation of lattice masses has basically shifted the HRG curve by 30 MeV towards higher temperatures. This can be clearly seen in the right panel of Fig. 1 where we plot the HRG curve with physical masses (dashed line) and compare it with the lattice data, where we have shifted all the points below 206 MeV temperature by 30 MeV, and the 209 MeV point by 15 MeV, towards lower temperature. Now the data points which agreed well with the HRG curve with lattice masses, agree well with the HRG curve with physical masses. Thus we propose that deviation from the continuum limit for the p4 data at low temperatures can be accounted for by shifting the data points by 30 MeV to lower temperature. For further confirmation of this procedure we also plot the recent HISQ result of c_{20} [5] in Fig. 1 (right): At low temperatures the shifted p4 data agree with the HISQ data. In the strange sector the discretization effects are slightly smaller than shown in Fig. 1. However, for simplicity we use the same shift of 30 MeV for all the coefficients.

We parametrize the shifted data using an inverse polynomial of three (c_{20}), four (c_{11} and c_{02}), or five (fourth and sixth order coefficients) terms:

$$c_{ij}(T) = \frac{a_{1ij}}{T^{n_{1ij}}} + \frac{a_{2ij}}{T^{n_{2ij}}} + \frac{a_{3ij}}{T^{n_{3ij}}} + \frac{a_{4ij}}{T^{n_{4ij}}} + \frac{a_{5ij}}{T^{n_{5ij}}} + c_{ij}^{\rm SB}, \qquad (2)$$

where $c_{ij}^{\rm SB}$ is the Stefan-Boltzmann value of the particular coefficient, and the powers n_{kij} are required to be integers between 1 and 42. As in our parametrization of the EoS at zero net baryon density [3], we match this parametrization to the HRG value at temperature $T_{\rm SW}$ by requiring that the Taylor coefficient and its first and

second derivatives are continuous. Since the recent lattice data obtained using HISQ action [5] shows that the second order coefficients approach their Stefan-Boltzmann limits slowly, we require that their value is 95% of their Stefan-Boltzmann value at 800 MeV temperature. These constraints fix three (or four) of the parameters a_{kij}. The remaining parameters, including the switching temperatures, are fixed by a χ^2 fit to the lattice data. As an example we show the parametrized c_{20} in the right panel of Fig. 1.

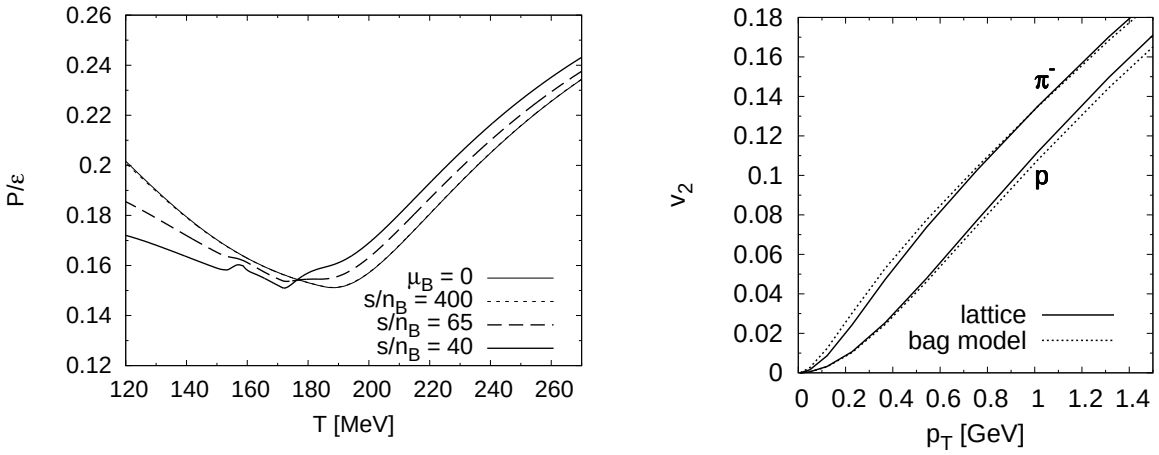

Figure 2. (Left) Pressure over energy density as function of temperature on various isentropic curves with constant entropy per baryon.
(Right) p_T-differential elliptic flow of pions (upper curves) and protons (lower curves) in an ideal fluid simulation of $\sqrt{s_{\rm NN}} = 17$ GeV Pb+Pb collisions at $b = 7$ fm.

Once the coefficients are known, pressure can be written as

$$\frac{P}{T^4} = \sum_{ij} c_{ij}(T) \left(\frac{\mu_B}{T}\right)^i \left(\frac{\mu_S}{T}\right)^j, \tag{3}$$

and all the other thermodynamical quantities can be obtained from Eq.(3) by using the laws of thermodynamics. As pressure at $\mu_B = 0$, i.e. the coefficient c_{00}, we use our earlier parametrization $s95p$-v1 [3]. We describe the EoS in the left panel of Fig. 2 by showing the pressure to energy density ratio on various isentropic curves with constant entropy per baryon. The curves at $s/n_B = 400$, 65, and 40 are relevant at collision energies $\sqrt{s_{\rm NN}} = 200$, 39 and 17 GeV, respectively. At $s/n_B = 400$ (dotted line), the EoS is basically identical to the EoS at $\mu_B = 0$ (thin solid line). This vindicates the common approximation of ignoring the finite net baryon density in the description of collisions at the full RHIC energy ($\sqrt{s_{\rm NN}} = 200$ GeV). At larger baryon densities the effect of finite baryon density is no longer negligible. The larger the density, the stiffer the EoS above, and softer below the transition temperature. Furthermore, additional structure begins to appear around the transition temperature with increasing density. This structure is mostly an unphysical artefact of our fitting procedure. We required the two first derivatives with respect to temperature to be continuous, but the speed of sound is proportional to the second derivative of the coefficients. Thus, in our parametrization, the derivative of the speed of sound is not continuous, and ripples may appear at a

switching temperature of any coefficient. Nevertheless, when pressure is plotted as a function of energy density, these structures are hardly visible. Therefore we do not expect them to affect the buildup of flow and the evolution of the system, and consider our parametrization a reasonable first attempt. The work to obtain a smoother and better constrained parametrization is in progress.

We illustrate the effect of the EoS on flow by studying elliptic flow in Pb+Pb collision at the full SPS collision energy ($\sqrt{s_{\rm NN}}$ = 17 GeV). For simplicity we use a boost invariant ideal hydrodynamical model to compare our lattice based EoS to a bag model EoS with a first order phase transition. We tune the calculation to reproduce the NA49 data for negative hadrons and net protons in the most central collisions [6], and use freeze-out temperatures of $T_{\rm dec}$ = 130 and 120 MeV for the lattice and bag model EoSs, respectively. Since it is very difficult to reproduce the elliptic flow data at SPS using ideal hydrodynamics, we do not try to fit the data. Instead we calculate the p_T-differential v_2 of pions and protons at fixed impact parameter of b = 7 fm, see the right panel of Fig. 2. At RHIC, the pion $v_2(p_T)$ is insensitive to the EoS, but the proton $v_2(p_T)$ shows a clear dependence on it [7]. However, at lower collision energy the behaviour is different: Proton $v_2(p_T)$ is as insensitive to the EoS as the pion $v_2(p_T)$. This behaviour is supported by the early ideal fluid calculations of v_2: It was seen that at SPS both a bag model EoS and a purely hadronic EoS led to quite a similar $v_2(p_T)$ [8], but at RHIC a purely hadronic and lattice EoS led to a similar proton $v_2(p_T)$, whereas the bag model EoS lead to a smaller proton $v_2(p_T)$ [7].

To summarise, we have shown that a temperature shift of 30 MeV is a good approximation of the discretization effects in the lattice QCD data obtained using p4 action. We have constructed an equation of state for finite baryon densities based on hadron resonance gas and lattice QCD data. At the full SPS energy ($\sqrt{s_{\rm NN}}$ = 17 GeV) the p_T-differential elliptic flow is almost insensitive to the equation of state. This is bad news for the experimental search of the critical point, since a change from a first order phase transition to a smooth crossover does not cause an observable change in the flow.

Acknowledgments

This work was supported by BMBF under contract no. 06FY9092, and by the U.S. Department of Energy under contract DE-AC02-98CH1086.

References

[1] C. Miao *et al.* [RBC-Bielefeld Collaboration], PoS **LATTICE2008** (2008) 172.
[2] M. Cheng *et al.*, Phys. Rev. D **79** (2009) 074505.
[3] P. Huovinen, P. Petreczky, Nucl. Phys. **A837** (2010) 26-53.
[4] P. Huovinen, P. Petreczky, J. Phys. Conf. Ser. **230** (2010) 012012.
[5] A. Bazavov *et al.* [HotQCD Collaboration], J. Phys. Conf. Ser. **230** (2010) 012014.
[6] P. G. Jones *et al.* [NA49 Collaboration], Nucl. Phys. **A610** (1996) 188C-199C.
[7] P. Huovinen, Nucl. Phys. **A761** (2005) 296-312.
[8] P. F. Kolb, P. Huovinen, U. W. Heinz, H. Heiselberg, Phys. Lett. **B500** (2001) 232-240.